# Model-based algorithms for phenotyping from 3D imaging of dense wheat crops

Andrew Thompson, Valerie Livina, Peter Harris, Imran Mohamed and Richard Dudley
National Physical Laboratory, Hampton Road, Teddington, TW11 0LW, United Kingdom

***Abstract*—High-throughput phenotyping requires the automation of the process of extracting relevant quantitative information from crop images. We achieve this goal for dense wheat crops by applying model-based data analysis techniques (including clustering and data-fitting) to high-resolution 3D point clouds obtained from structured light laser scanners. By performing experiments comparing our estimates of crop height, spike height and spike width with manual measurements, we demonstrate that our approach is promising even in the challenging context of dense vegetation.**

***Index Terms*—Phenotyping, wheat, feature extraction, clustering, data-fitting.**

## I. Introduction

Plant phenotyping refers to the measurement of the structural and functional properties of plants. For wheat, phenotypes of interest include crop height, ear size and yield. Phenotype data is used to guide cross-breeding programmes for new varieties and an efficient process requires large phenotype data sets, recorded in a quantifiable and accurate way [1]. Phenotype data ideally should take place in-situ on outdoor plots with variations in location, soil type, drainage etc. Capturing data for wheat ear size currently relies on manual sampling with a ruler [2]. Measurements are repeated on hundreds of plots in the same field, each growing different wheat varieties. Data collection is time-consuming, and the quality of the data limited by the sample size within each plot, creating a data bottleneck in capacity.

An alternative approach is to obtain measurements indirectly by analysing images. In this paper, we study how 3D point clouds obtained from structured light laser scanners can be analysed to extract useful information. 3D images were obtained using a *Photoneo PhoXi 3D* structured light laser scanner [3], which uses a moving pattern of stripes projected onto a scene using a high-brightness laser. A CCD camera captures the changing patterns on the scene and converts the distortions around surfaces directly into a point cloud. Imaging of field grown crop plots is much faster than taking manual measurements, thereby expanding the quantity of data that can be collected. For the approach to be efficient in its entirety, it is also vital that feature extraction is fully automated, which requires suitable data analysis algorithms. In addition, in order to perform high throughput phenotyping in a realistic in situ environment, it is crucial to have algorithms designed to make sense of dense vegetation.

There is now a significant literature on feature detection from 3D point clouds, see for example [4] for a survey of segmentation methods for point clouds. Such techniques have previously been applied in the context of detecting phenotyping traits of maize [5], strawberry plants [6] and sunflower plants [7], mostly in non-dense settings, using a variety of imaging methods such as Multiview Stereovision (MVS) and Structure from Motion (SfM), and most popularly LiDAR. Where our approach differs from this prior work is in taking on the challenge of a dense crop environment. The most closely related work we aware of is [8] in which wheat spikes are detected from dense environments using mean shift segmentation and voxel-based connected component analysis, though estimates of spike heights and widths are not considered. It is also worth mentioning that an even greater volume of work exists on detecting phenotyping traits (including for wheat) from standard 2D images, though the algorithms required are very different.

In summary, the objective of this work is to demonstrate how algorithms can be used to extract features of phenotypic interest from 3D point cloud images of dense wheat crops. We describe the model-based algorithms that we use, and we also present the results of two different experiments designed to evaluate the effectiveness of our approach.

## II. Feature extraction algorithms

Our feature extraction algorithms have two main building blocks: the DBSCAN [9] clustering algorithm and least-squares curve fitting. We describe these two building blocks.

### A. Clustering using DBSCAN

Central to feature extraction from 3D imaging is segmentation of the point clouds into biologically significant regions. Individual crops must first be separated, then wheat spikes must be identified, after which spikelets must be identified within the wheat spikes.

The task of segmenting a 3D point cloud is essentially one of clustering points in 3D space. Many different clustering algorithms exist, and they vary according to the cluster model on which they are based. We found that the density-based DBSCAN (Density Based Spatial Clustering of Applications with Noise) algorithm [9] was well suited to the task and performed better than the popular centroid-based $K$-means approach [10]. It has the advantages that the number of clusters does not need to be specified in advance, and it is able to identify clusters of different sizes and shapes.

DBSCAN works by first identifying the *core points* of the data set, that is those with at least $k$ neighbours, where points are defined to be neighbours if they are within a Euclidean

distance $\epsilon$. The core points are then grouped into maximal clusters such that each core point has a neighbour in the same cluster. All other points are then either assigned to the nearest cluster (if the distance to some point is less than $\epsilon$) or otherwise designated as outliers. DBSCAN therefore has two parameters $k$ and $\epsilon$ which must be tuned carefully by a domain expert.

A naïve implementation of DBSCAN has complexity $\mathcal{O}(n^2)$, where $n$ is the number of data points. If, however, spatial partitioning is used for the nearest neighbour search, the complexity can be reduced to $\mathcal{O}(n \log n)$. We used MATLAB code for DBSCAN provided by [11] which makes use of a $k$-$d$ trees spatial partitioning algorithm coded in C++ provided by [12].

### B. Least-squares curve fitting

Least-squares curve fitting is used to characterize clusters found using DBSCAN by fitting a curve of best bit to the central axis of each cluster. In particular, it can be used to separate spikes from stems, and to estimate the width and height of spikes.

Given a cluster consisting of $n$ points, and denoting by $\{x_i\}$, $\{y_i\}$ and $\{z_i\}$ the $x$, $y$ and $z$ coordinates of point $i$ for $i \in \{1, \ldots, n\}$, our approach was to fit a quadratic in $z$ to both the $x$ and $y$ coordinates. Parametrising in terms of the $z$ coordinate makes sense since we expect the axis of each spike to be well-aligned with the $z$ axis. Other parametrisations are possible, such as modelling each of $x$, $y$ and $z$ as a polynomial in a vector of latent variables corresponding to each point, but this approach is more computationally intensive. For the $x$ coordinates we solve

$$\min_{a,b,c} \sum_{i=1}^{n} [x_i - (az_i^2 + bz_i + c)]^2,$$

and for the $y$ coordinates we solve

$$\min_{p,q,r} \sum_{i=1}^{n} [y_i - (pz_i^2 + qz_i + r)]^2.$$

### C. Features extracted

In this paper we describe the extraction of the following three features for each wheat crop:

1) Maximum height of crop above the ground.
2) Length of wheat spike.
3) Maximum diameter of wheat spike.

Crop height can be determined after clustering by examining the $z$ coordinates of each of the clusters. Length and diameter of wheat spikes can be obtained from the least-squares fits. More precisely, spike length is found by integrating along the quadratic curve between the minimum and maximum $z$ coordinates. Meanwhile, maximum diameter of a spike is estimated by analyzing the deviations of the points from the curve of best fit.

## III. Experimental design

Two experiments were performed to investigate the accuracy of data analysis algorithms for extracting features from dense wheat crops. In both cases dense wheat crops were imaged using a *Photoneo PhoXi 3D* structured light laser scanner [3].

Fig. 1: The arrangement of 25 wheat stems in Experiment 1. Also visible is the calibration plate used by the laser scanner device.

### A. Experiment 1

The aim of the first experiment was to compare the results of feature extraction with manual measurements. Harvested wheat crops were selected and the manual measurements described in Section II-C were taken. Wheat crops were arranged in a square grid in an indoor laboratory with stem bases at the same horizontal height. Two grids were investigated:

- 9 stems in a 3x3 grid arrangement, with grid squares of side length 5 cm.
- 25 stems in a 5x5 grid arrangement, with grid squares of side length 2.5 cm.

The 25-stem arrangement and the laboratory environment is shown in Figure 1.

3D point cloud images were generated from three directions, roughly 120° apart. The three point clouds for each image were then merged in MATLAB. We then ran our feature extraction toolbox on the merged point clouds and extracted the desired features.

### B. Experiment 2

We also obtained qualitative evidence concerning the ability of our algorithms to function well in a more realistic (and challenging) outdoor scenario. A 2 m x 2 m wheat trial plot was built, enclosed by two linear motion rails and two A-frame camera mounts. The rails were placed on the north and south side of the plot to allow the A-frames to move in an east-west direction. 3D point cloud images were generated from eight directions, roughly 45° apart. The eight point clouds for each

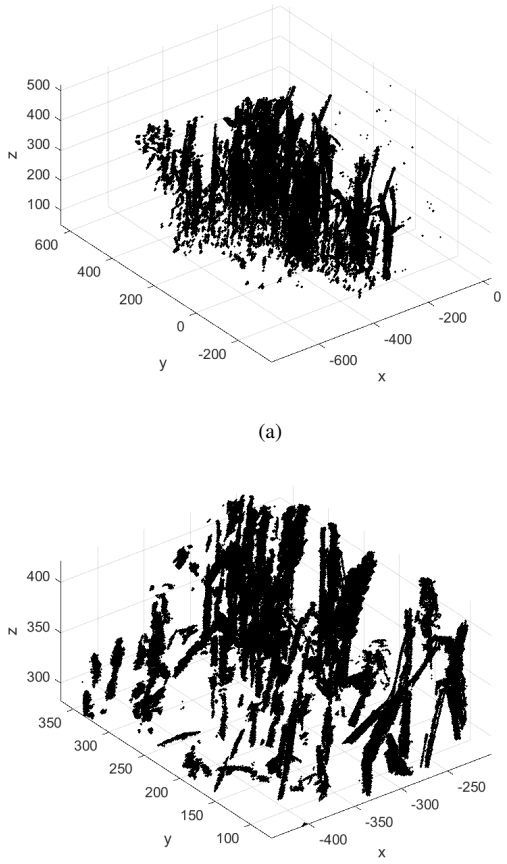


(a)

(b)

Fig. 2: (a) The initial point cloud for Experiment 2; (b) Zooming in on part of the same point cloud to display detail.

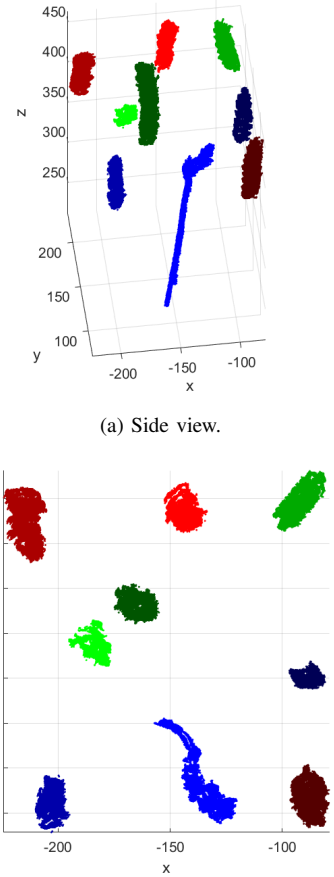


(a) Side view.

(b) Top view.

Fig. 3: Result of ear detection with 9 wheat crops.

image were then merged in MATLAB. Figure 2 shows the initial point cloud, along with a zoomed-in image displaying more detail.

As in Experiment 1, we then ran our feature extraction toolbox on the merged point clouds and qualitatively explored the ability of our algorithms to segment the crops and locate spikes.

Obtaining 3D images of wheat outdoors is challenging. Variable lighting conditions and wind influence the quality of the image and/or the ability of the instrument to acquire an image. The scanner's acquisition time of 1 to 2 seconds meant that care was required to perform image capture when the wheat was stationary. Moreover, crop segmentation and spike location is more challenging since a natural spatial distribution of wheat crops is more variable than the controlled scenario of Experiment 1, which means that scan visibility is reduced and segmentation of crops is more challenging.

## IV. Results

### A. Experiment 1

We ran our feature extraction toolbox with default parameter settings on the 3x3 arrangement. We were able to determine the correct number of ears (nine) using the DBSCAN clustering algorithm and least-squares data fitting. Figure 3 displays the result of the ear detection, viewed from both a horizontal and vertical direction. In this and all subsequent plots, $x$, $y$ and $z$ are in mm and refer to the coordinates defined by the 3D camera. Ear detection was somewhat successful, although one of the clusters obtained still included the stem. A full comparison of stem height, ear length and ear width are given in Table I.

Estimates of crop height are the most accurate in relative terms. Interestingly, there is a strong relative bias between the manual and the analysis crop height values: all of the analysis values are 0.7 cm less than the corresponding manual values. We believe that the analytic calculation is actually the more accurate, and the discrepancy is due to a bias in the manual measurements.

Our algorithms currently find the estimation of spike length the most challenging. The RMSE is extremely high (6.16 cm), although this large value is due in large part to a single crop in which the spike was incorrectly determined to be a large part of the stem. If this data item is removed from the calculation, the RMSE reduces to 1.81 cm (scaled RMSE of 25.3%). With the exception of the data item just mentioned, the algorithm consistently underestimates spike length, due to only finding

| Stem number | Crop height (cm) | | Spike length (cm) | | Spike diameter (mm) | |
|---|---|---|---|---|---|---|
| | Manual | Analysis | Manual | Analysis | Manual | Analysis |
| 1 | 46.0 | 44.86 | 8.2 | 7.82 | 12 | 10.30 |
| 2 | 48.0 | 46.28 | 8.5 | 6.58 | 11 | 8.12 |
| 3 | 43.5 | 42.74 | 7.6 | 3.37 | 12 | 11.39 |
| 4 | 46.5 | 45.23 | 10.0 | 9.82 | 10 | 9.88 |
| 5 | 47.0 | 45.52 | 8.6 | 7.86 | 12 | 7.74 |
| 6 | 46.0 | 44.70 | 6.5 | 6.36 | 10 | 5.87 |
| 7 | 44.5 | 43.40 | 6.1 | 4.80 | 8 | 6.86 |
| 8 | 46.0 | 44.80 | 6.7 | 24.46 | 12 | 8.46 |
| 9 | 46.0 | 45.06 | 10.1 | 8.58 | 11 | 9.30 |
| RMSE | 1.24 | | 6.16 | | 2.66 | |
| Scaled RMSE | 2.7% | | 75.6% | | 24.2% | |

TABLE I: Estimation comparisons for crop height, spike length and spike diameter, with the 9 crop arrangement.

a section of the spike. This in turn is due to a combination of limited scan visibility and algorithm inaccuracy.

Estimates for maximum spike diameter are reasonably good. A bias can be observed: the analysis values usually underestimate the width (here the manual estimate can be trusted to within an accuracy of 1 mm). The underestimate is most likely due to a combination of limited scan visibility, and the fact that points in low-density regions on the extremities of the spike are often removed in the DBSCAN clustering algorithm. One possible way to mitigate this effect and potentially obtain more accurate diameter estimates would be to include a postprocessing step which reassigns the original points to the obtained clusters, and this is left as future work.

Figure 4 displays the result of the spike detection for the 25 crop arrangement, viewed from both a horizontal and vertical direction. For this experiment, running our algorithms with default settings did not return the exact number of spikes. 22 spikes were found, with one spike (number 21) missing, three pairs of spikes merged (numbers 1 and 14, numbers 3 and 12, numbers 11 and 15) and one spike split in two (number 16). It is possible that better results could be obtained by adjusting the parameters.

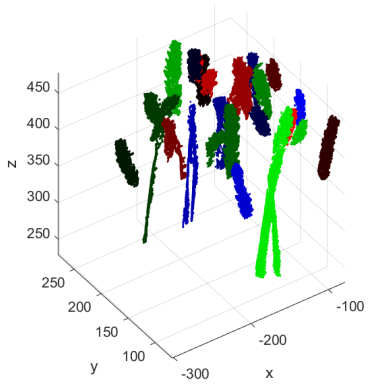


(a) Side view.

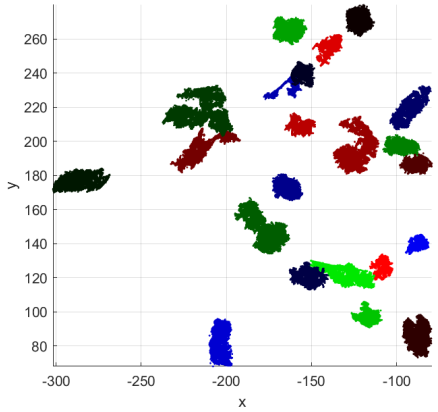


(b) Top view.

Fig. 4: Result of spike detection with 25 wheat crops.

### *B. Experiment 2*

We ran our feature extraction toolbox with default parameter settings on the merge point cloud from the outdoor image acquisition. Figure 5(a) shows the result of segmenting the crops using DBSCAN. Different colours represent different obtained clusters. We observe qualitatively that the algorithm is able to segment the point cloud into individual crops successfully. Figure 5(b) shows the result of refining the clusters using least-squares curve fitting. We observe that many wheat spikes have been identified, and that almost all of the remaining clusters are indeed wheat spikes.

## V. Estimation of Crop Yield

In this section, we outline two approaches for estimating the total volume of grain in a wheat crop scene.

1) In the first approach, we model the volume of grain in a wheat spike as being a fixed fraction of the volume of its enclosing cylinder. An estimate for the volume of the enclosing cylinder can be obtained from the estimates for diameter and length described in Sections II and IV.
2) In the second approach, we further use DBSCAN to cluster the point clouds for each wheat spike into spikelets. The volume estimate is then obtained by modelling each spikelet as an ellipsoid and calculating its minimum enclosing ellipsoid.

Figure 6 illustrates both approaches to estimating grain volume.

## VI. Conclusion

We have described model-based algorithms for feature extraction from 3D point clouds of wheat crops. Our results

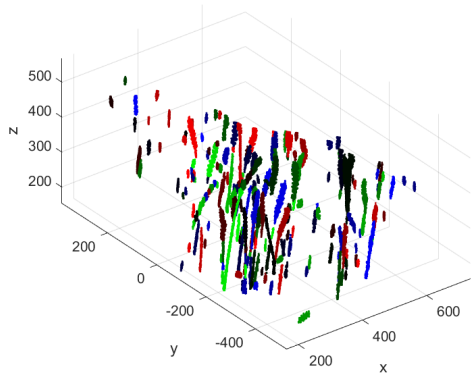


(a) Stem segmentation.

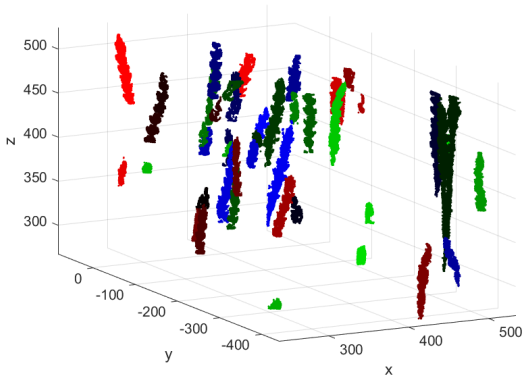


(b) Spike detection.

Fig. 5: Result of clustering and refining the point clouds from the outdoor imaging.

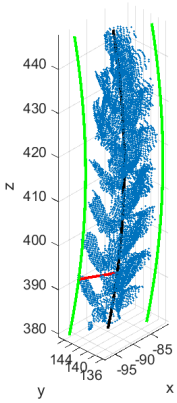


(a) Fitting an enclosing cylinder to one of the wheat spikes in Experiment 1: the curve of best fit is shown in black, maximum radius is shown in red, and the enclosing cylinder in the plane of the maximum radius is shown in green.

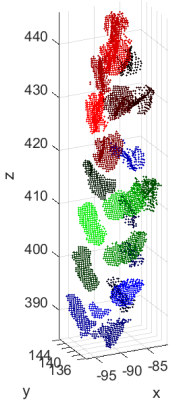


(b) DBSCAN clustering to separate the same spike into spikelets: spikelets are shown in different colours.

Fig. 6: An illustration of two approaches to estimating crop yield.

demonstrates clearly the potential of our algorithms to identify phenotyping traits even from dense wheat crops.

## Acknowledgments

This work is supported by the UK Government's Department of Business, Energy and Industrial Strategy (BEIS).

## References

[1] J. L. Araus and J. E. Cairns, "Field high-throughput phenotyping: the new crop breeding frontier," *Trends in Plant Science*, vol. 19, no. 1, pp. 52–61, 2014.

[2] A. Torres and P. Julian, *Crop morphological traits*. CIMMYT, 2012, ch. 19.

[3] Photoneo, "PhoXi 3d scanner," https://www.photoneo.com/phoxi-3d-scanner/.

[4] A. Nguyen and B. Le, "3D point cloud segmentation: A survey," in *2013 6th IEEE Conference on Robotics, Automation and Mechatronics (RAM)*, 2013, pp. 225–230.

[5] Q. Qiu, N. Sun, Y. Wang, Z. Fan, Z. Meng, B. Li, and Y. Cong, "Field-based high-throughput phenotyping for maize plant using 3D lidar point cloud generated with a phenomobile," *Frontiers in Plant Science*, vol. 10, p. 554, 2019.

[6] J. Q. He, R. J. Harrison, and B. Li, "A novel 3D imaging system for strawberry phenotyping," *Plant Methods*, vol. 13, no. 1, p. 93, 2017.

[7] W. Gélard, M. Devy, A. Herbulot, and P. Burger, "Model-based segmentation of 3D point clouds for phenotyping sunflower plants," in *12th International Joint Conference on Computer Vision, Imaging and Computer Graphics Theory and Applications (VISAPP 2017)*, vol. 4, 2017, pp. 459–467.

[8] K. Velumani, S. O. Elberink, M. Y. Yang, and F. Baret, "Wheat ear detection in plots by segmenting mobile laser scanner data," *ISPRS Annals of Photogrammetry, Remote Sensing & Spatial Information Sciences*, vol. 4, 2017.

[9] M. Ester, H.-P. Kriegel, J. Sander, and X. Xu, "A density-based algorithm for discovering clusters in large spatial databases with noise," in *Knowledge Discovery in Databases (KDD)*, vol. 96, no. 34, 1996, pp. 226–231.

[10] S. Lloyd, "Least squares quantization in PCM," *IEEE Transactions on Information Theory*, vol. 28, no. 2, pp. 129–137, 1982.

[11] R. Harkes, "Fast DBSCAN using kdtrees," https://uk.mathworks.com/matlabcentral/fileexchange/68482-fast-dbscan-using-kdtrees, 2018.

[12] A. Tagliasacchi, "kdtree," https://github.com/ataiya/kdtree/, 2017.